X-Band EPR Studies of Ferroelectric Lead Titanate (PT), Piezoelectric Lead Magnesium Niobate (PMN), and PMN/PT Powders at 10 and 85 K

Jiong Huang, N. Dennis Chasteen,*,† and John J. Fitzgerald*

Department of Chemistry and Biochemistry, South Dakota State University, Brookings, South Dakota 57007, and Department of Chemistry, University of New Hampshire, Durham, New Hampshire 03824

Received March 31, 1998. Revised Manuscript Received September 24, 1998

X-band EPR spectra of lead titanate (PT) and lead magnesium niobate (PMN) powders prepared by different synthetic methods and a PMN/PT powder of the composition 0.9 PMN/0.1 PT were obtained at 85 and 10 K. Several EPR signals due to adventitious Fe^{3+} ion impurities, a signal due to the Ti^{3+} ion, and a signal due to the Pb^{3+} ion are observed for PT, PMN, and PMN/PT powders. The EPR signals observed at $g = 2.0$ and 6.0 are assigned to Fe^{3+} ions in the B-sites of the perovskite lattice structure of lead titanate with axial symmetry. The EPR signals observed at $g = 1.99$ and 4.25 are assigned to Fe^{3+} ions in the B-sites of the perovskite lattice structure of PMN and 0.9 PMN/0.1 PT materials with cubic and rhombic symmetries, respectively. The sharp EPR signal observed at $g = 1.94$ is assigned to Ti^{3+} ion for PT and 0.9 PMN/0.1 PT powders. In addition, a broader EPR signal at $g = 2.28-2.30$ for PMN obtained by the molten salt method is assigned to axial Pb^{3+} ion sites in this PMN material. EPR results obtained here for the Fe^{3+} ions in the B-sites of the PMN materials, in particular, suggest that both cubic and rhombic symmetry sites corresponding to a range of $Nb(OMg)_x(ONb)_{6-x}$ site configurations exist in the PMN. These EPR results indicate that PMN likely exists with partial B-site cation (Mg/Nb) ordering in the perovskite lattice structure.

Introduction

The dielectric properties of the complex lead-based perovskite materials with the general formula $Pb(B'_x B''_{1-x})O_3$ are dependent on chemical ordering in the cation B-sites.[1,2] Many complex perovskites ($PbB'_{1/3}Nb_{2/3}O_3$, where $B' = Zn^{2+}$, Mg^{2+}, and $PbB'_{1/2}B''_{1/2}O_3$, where $B' = In^{3+}$, $B'' = Nb^{5+}$ and $B' = Sc^{3+}$, $B'' = Nb^{5+}$ or Ta^{5+}) have shown both short-range and long-range B-site cation ordering.[3−12] If the B-sites are randomly occupied, e.g., lead zirconate titanates (PZTs), such perovskites will exhibit normal ferroelectric or antiferroelectric properties.[13] Lead-based perovskites with B-site cation ordering with short coherency (2−50 nm), however, are relaxor ferroelectrics (relaxors) that exhibit broad, diffuse phase transitions instead of the sharply defined Curie transition temperatures observed for normal ferroelectrics. Abnormally high dielectric constants are observed over a wide temperature range for these relaxor materials. The temperature where the dielectric constant is maximum (T_M) shifts to higher temperature and decreases in magnitude with increasing frequency. In relaxor ferroelectrics, the structural disorder in the B-sites has been proposed to disrupt the translational crystal symmetry, giving the lattice structure an apparent anisotropic component for some measured electrical properties.[14−15]

Lead magnesium niobate, $Pb(Mg_{1/3}Nb_{2/3})O_3$ (PMN), a nonstoichiometric B′B″ lead perovskite with short, coherent long-range order on the nanoscale (40−100 Å), is a relaxor ferroelectric system, containing both Mg-rich and Nb-rich regions.[16−19] A schematic representation of the A(Pb^{2+})- and B(Nb^{5+} or Mg^{2+})-sites in PMN is shown in Figure 1. While PMN undergoes a diffuse

* To whom correspondence should be addressed.
† University of New Hampshire.

(1) Cross, L. E. *Ferroelectrics* **1994**, *151*, 305.
(2) Ye, Z.-G. *Ferroelectrics* **1996**, *184*, 193.
(3) Galasso, F. S. *Structure, Properties and Preparation of Perovskite-Type Compounds*; Pergamon Press: Oxford, 1963.
(4) Galasso, F.; Pyle, J. *Inorg. Chem.* **1963**, *2*, 482.
(5) Randall, C. A.; Bhalla, A. S.; Shrout, T. R.; Cross, L. E. *J. Mater. Res.* **1990**, *5*, 829.
(6) Cross, L. E. *Ferroelectrics* **1987**, *76*, 241.
(7) Smolenskii, G. A.; Agronovskaya, A. I. *Sov. Phys. Sol. State* **1959,** *1*, 1429.
(8) Viehland, D.; Jang, S. J.; Cross, L. E.; Wuttig, M. *J. Appl. Phys.* **1990**, *68*, 2916.
(9) Viehland, D.; Jang, S. J.; Cross, L. E.; Wuttig, M.*J. Appl. Phys.* **1991**, *69*, 414.
(10) Hilton, A. D.; Randall, C. A.; Barber, D. J.; Shrout, T. R. *Ferroelectrics* **1989**, *93*, 379.
(11) Chen, J.; Chan, H. M.; Harmer, M. P. *J. Am. Ceram. Soc.* **1989**, *72*, 593.
(12) Hilton, A. D.; Barber, D. J.; Randall, C. A.; Shrout, T. R. *J. Mater. Sci.* **1990**, *25*, 3461.
(13) Glazer, A. M.; Mabud, S. A. *Acta Cryst.* **1978**, *B34*, 1060.
(14) Gupta, S. M.; Kulkarni, A. R. *Mater. Chem. Phys.* **1994**, *39*, 98.
(15) Zhukov, S. G.; Chernyshev, V. V.; Aslanov, L. A.; Vakhrushev, S. B.; Schenk, H. *J. Appl. Crystallogr.* **1995**, *28*, 385.
(16) Bursill, L. A.; Qian, H.; Peng, J.; Fan, X. D. *Physica B* **1995**, *216*, 1.
(17) Prouzet, E. Husson, E.; de Mathan, N.; Morell, A. *J. Phys.: Condens. Matter* **1993**, *5*, 4889.
(18) Zhang, Q. M.; You, H.; Mulvihill, M. L.; Jang, S. J. *Solid State Commun.* **1996**, *97*, 693.
(19) Husson, E.; Chubb, M.; Morell, A. *Mater. Res. Bull.* **1988**, *23*, 357.

10.1021/cm980206n CCC: $15.00
Published on Web 11/21/1998

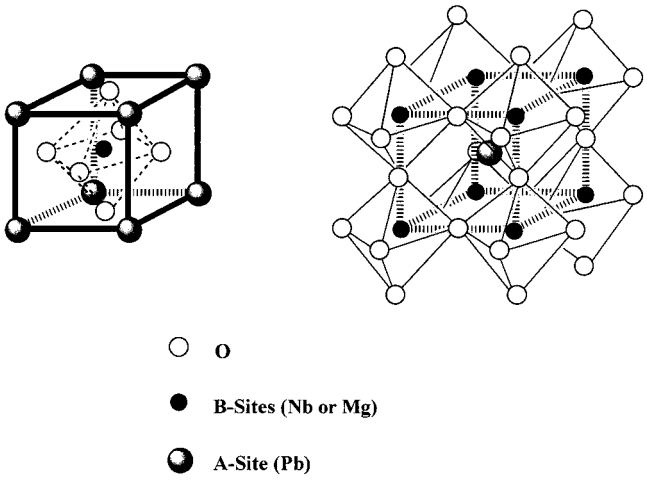

Figure 1. Schematic representation of the idealized A- (Pb^{2+}) and B- (Nb^{5+} or Mg^{2+}) sites in the perovskite lattice structure for $Pb(Mg_{1/3}Nb_{2/3})O_3$ (PMN).

phase transition with a maximum T_M near −7 to −15 °C, additions of lead titanate (PT) increase T_M by about 5 °C/mol %. PMN and PMN/PT binary systems in the 100−66 PMN/0−34 PT mol % region are relaxor ferroelectrics that exist in a perovskite superlattice structure.[20,21] Alloys containing greater than 34 mol % PT, the morphotropic phase boundary (MPB), are normal ferroelectrics. The PMN-rich ceramics in the PMN/PT system are characterized by not only high dielectric constants but also large electrostrictive effects. Because of the magnitude and diffuse nature of the dielectric maximum and the high values for strain introduced by electrostriction, PMN/PT ceramics containing 10 mol % PT are ideal for use as ceramic capacitors and electrostrictive precision actuators and micropositioners. Compositions of PMN/PT near the MPB exhibit dielectric and pyroelectric anomalies at the two temperatures for rhombohedral−tetragonal and tetragonal−cubic phase lattice structure transitions.

The different local B-site cation distortions and the unknown nature of the B′B″ chemical ordering found in the B-sites of PMN and PMN/PT materials having a perovskite lattice structure have been postulated to provide a mechanism for the high dielectric and electrostrictive properties observed for these systems.[2] Numerous physical−chemical techniques have been used to study the local B-site distortions, including X-ray and neutron diffraction,[18,22−25] XPS,[26] EXAFS,[17] EPR,[27,28] HRTEM,[16] and Raman[29,30] and NMR spectroscopy.[31,32] Two important structural features observed for PMN and PMN/PT systems from these studies likely provide atomic-level explanations for the high dielectric properties of PMN in the perovskite lattice structure phase: (1) long-range B-site lattice distortions may occur causing deviations from cubic crystal symmetry at low temperature, and (2) short-range B-site cation changes involving off-center shifts or movement in the six-coordinate (octahedral) B-site oxide lattice holes. These short- and long-range structural changes are postulated to cause a separation of the local positive and negative charge in these materials that creates a bulk spontaneous polarization. In addition to these structural changes, complex multiple B-site perovskites, such as PMN, have been postulated to contain chemical disorder of the two cations in the B-sites due to a random or partially disordered distribution of Mg^{2+} and Nb^{5+} ions in the B-sites that leads to local nanoregions of variable Mg/Nb ratios. These nanoscale domain regions likely produce uncompensated charge domains, thereby increasing the content of polar domain regions.[2]

Previous spectroscopic studies, however, have not provided a complete detailed understanding of the role of the short-range B-site ordering in the overall chemical structure of PMN that can provide an atomic-level explanation for the relaxor ferroelectric behavior of PMN.[2,33] Conclusions about the short-range B-site ordering from these research efforts have been controversial. Studies using HRTEM,[16] EXAFS,[17] and single-crystal X-ray diffraction[18] have suggested that two B-site nanodomains exist in the perovskite lattice structure of PMN. The first type of nanodomain is the so-called "1:1 ordered" regions, where Mg and Nb ions are arrayed in a successive or alternating order (Mg−O−Nb) with a Mg/Nb mole ratio of 1:1. Such "Mg^{2+}-rich" regions, with the proposed composition of $[Pb_2MgNbO_6]^-$, are postulated to be negatively charged and nonstoichiometric and must be compensated for by a surrounding positively charged "Nb^{5+}-rich" region of Nb−O−Nb ordering with a composition of $[PbNbO_3]^+$ to maintain charge neutrality.[34] The majority of spectroscopic studies to date have supported this model.[16−19] However, recent static ^{93}Nb NMR measurements for single crystals of PMN found that the observed ^{93}Nb resonance shows both a fast- and slow-relaxing component. This behavior was interpreted as being inconsistent with the predicted 1:1 "ordered" Mg/Nb model for PMN.[32] The XPS results of Parmigiani et al.[26] were also interpreted as lacking in experimental support for the large charge fluctuations predicted by the 1:1 model. Such results, however, indicated that the cation ordering in the B-site is of a more complex nature and that the Mg and Nb ions are more likely randomly distributed. The charge neutrality of the bulk material would then be maintained by the presence of lead and/or oxygen vacancies. Depero and Sangaletti also proposed

(20) Choi, S. W.; Shrout, T. R.; Jang, S. J.; Bhalla, A. S. *Mater. Lett.* **1989**, *8*, 253.
(21) Choi, S. W.; Shrout, T. R.; Jang, S. J.; Bhalla, A. S. *Ferroelectrics* **1989**, *100*, 29.
(22) Bonneau, P.; Garnier, P.; Calvarin, G.; Husson, E.; Gavarri, J. R.; Hewat, A. W.; Morell, A. *J. Solid State Chem.* **1991**, *91*, 350.
(23) De Mathan, N.; Husson, E.; Calvarin, G.; Gavarri, J. R.; Hewat, A. W.; Morell, A. *J. Phys.: Condens. Matter* **1991**, *3*, 8159.
(24) De Mathan, N.; Husson, E.; Calvarin, G.; Morell, A. *Mater. Res. Bull.* **1991**, *26*, 1167.
(25) Vakhrushev, S.; Zhukov, S.; Fetisov, G.; Chernyshov, V. *J. Phys.: Condens. Matter* **1994**, *6*, 4021.
(26) Parmigiani, F.; Rollandi, L.; Samoggia, G.; Depero, L. E. *Solid State Commun.* **1996**, *100*, 801.
(27) Dimza, V. I. *Phys. Stat. Sol. (a)* **1993**, *140*, 543.
(28) Glinchuk, M. D.; Skorokhod, V.; Bykov, I. P.; Dimza, V.; Černošková, E. *J. Phys.: Condens. Matter* **1994**, *6*, 3421.
(29) Idink, H.; White, W. B. *J. Appl. Phys.* **1994**, *76*, 1789.
(30) Husson, E.; Abello, L.; Morell, A. *Mater. Res. Bull.* **1990**, *25*, 539.
(31) Glinchuk, M. D.; Laguta, V. V.; Bykov, I. P. *Ferroelectrics* **1991**, *124*, 255.
(32) Glinchuk, M. D.; Bykov, I. P.; Laguta, V. V. *Ferroelectrics* **1993**, 143, 39.
(33) Depero, L. E.; Sangaletti, L. *Solid State Commun.* **1997**, *102*, 615.
(34) Newnham, R. E. *NIST Special Pub. 804*, **1991**, 39.

several new structural models for PMN based on computer simulations of detailed X-ray reflection data.[33] This work suggested that an average long-range cubic lattice structure for PMN is consistent with the X-ray reflection results, with the possible "intergrowth" of crystalline rhombohedral and tetragonal phases. However, the intergrowth of these two phases is only consistent with the temperature dependence for the long-range order in PMN but does not provide any further information relating to the short-range local B-site cation order that exists in PMN materials.

EPR spectroscopy, due to its high sensitivity to the local chemical environment of metal ions,[35] is an important approach to study both short-range distortions and/or cation site orderings for electronic materials of the perovskite lattice, as suggested from recent EPR studies on lead zirconate titanate (PZT), lead lanthanum zirconate titanate (PLZT), and PMN powders.[27−28,36−39] Extensive EPR studies have been reported for PT,[40] PZT,[36,39] and PLZT systems.[37,38] The EPR signals of several paramagnetic species have been observed and analyzed for these systems. In general, there are three types of Fe^{3+} ion signals (due to cubic, rhombic, and axial Fe^{3+} ion centers) observed for these systems. EPR signals due to Ti^{3+} ion in PT and PZT materials are usually observed at $g = 1.93$, while the EPR signal at $g = 2.00$ has been assigned to Pb^{3+} ions.[36−39] These studies thus provide a reference perspective from which the EPR investigations reported here for the less well-studied, yet important, PMN and PMN/PT systems may be understood.

An EPR study by Dimza for metal ion-doped PLZT and PMN materials, for example, has also shown that paramagnetic metal ion species contained in the B-sites of PMN and PLZT have related experimental EPR behavior from 273 to 418 K.[27] The interpretation of the EPR studies of the more thoroughly studied PLZT system, in particular, was most informative, suggesting the need for further detailed EPR studies of the PMN and PMN/PT systems.

Glinchuk and co-workers have recently reported a detailed EPR study of Fe^{3+} ions doped in PMN.[28] They conducted variable temperature EPR experiments and determined spin Hamiltonian zero-field splittings D and E from simulations using the following equation:

$$H = g\beta H + D[S_z^2 - 1/3\mathbf{S}(\mathbf{S}+1)] + E(S_x^2 - S_y^2) \quad (1)$$

where g is the electron spin factor, β is the Bohr magneton, S_x, S_y, and S_z are spin operators.

From these experiments, four EPR signals were identified due to different types of Fe^{3+} ion centers in the B-sites of PMN: a signal at $g = 4.3$ that was attributed to rhombic Fe^{3+} ion centers ($E/D = {}^1/_3$); stairlike bands between $g = 6$ and 8 that were assigned to axial Fe^{3+} ion centers ($E = 0$); a wide, intense line centered at $g = 2.0$, together with a weak low-field tailing signal at $g = 3.2$ observed at 475 K that was attributed to cubic Fe^{3+} ion centers caused by low symmetry cation fluctuations in the B-sites (D and E are close but not equal to zero); and a narrow $g = 2.0$ signal at 100 K that was believed to correspond to an ideal Fe^{3+} ion cubic center without local B-site fluctuations ($D = E = 0$). The hyperfine features of the latter resonance were interpreted as due to superhyperfine lines as a result of electron−nuclear interactions with the surrounding ^{207}Pb ions.

Detailed EPR studies of various PMN powders prepared by several important solid-state synthetic approaches and a related PMN/PT powder of the composition 0.9 PMN/0.1 PT are reported here in an effort to obtain a more complete understanding of the EPR behavior of these systems. The experimental EPR behavior of the PMN powders prepared by these different solid-state synthetic methods have been examined for two reasons: (1) different synthetic methods have been reported to cause substantial differences in the microstructure and local domain regions that occur in perovskite materials,[14,37,40] and (2) different synthetic methods used to prepare PMN powders have been reported to produce different final PMN products of variable contents of the PMN perovskite and/or pyrochlore phases.[14] The utility of EPR as a probe of the atomic-level changes in the local structure of the B-sites in the perovskite and/or pyrochlore phases of PMN and PMN/PT powders is demonstrated. To provide complete assignments for the observed EPR resonances for the PMN and PMN/PT systems, additional EPR measurements were also obtained for the related compounds, i.e., $PbTiO_3$, and the PMN pyrochlore phase of the formula $Pb_{1.83}Nb_{1.71}Mg_{0.29}O_{6.39}$.

Experimental Section

Reagents and Materials. PbO (Alfa, 99.9995%), Nb_2O_5 (Alfa, 99.9985%), TiO_2 (Anatase, Aldrich, 99.9+%), $PbTiO_3$ (Aldrich, 99+%), and $(MgCO_3)_4Mg(OH)_2{\cdot}5H_2O$ (Aldrich, 99%) were used as purchased. MgO (Aldrich, 99+%) was fired at 950 °C for 6 h prior to use.

Synthesis of PMN Powders. *1. Mixed Oxide Method.* The PMN powders were prepared using a two-step firing approach as reported by Gupta and Mulkarni.[14] MgO, PbO, and Nb_2O_5 powders were first mixed according to the PMN formula in an ethanol slurry for 1.5 h, the formed paste was dried in an oven (140 °C), and the resulting powder calcinated at 800 °C for 4 h. The resulting yellow powder was then mixed with 2 wt % poly(vinyl alcohol) binder and 1% excess PbO in ethanol for 1 h. After drying in an oven (140 °C), the mixture was pressed into pellets at 4000 psi using a Carver hydraulic press and fired at 900 °C for 4 h.

2. Columbite Method.[41] In this synthetic method, the columbite precursor $MgNb_2O_6$ was prepared by mixing MgO and Nb_2O_5 powders in ethanol for 1.5 h, drying of the solvent in an oven (140 °C), followed by firing of the powders at 1100 °C for 4 h. The resulting white powders were mixed with PbO according to the required PMN stoichiometry in ethanol for 1 h, followed by drying of the mixture in an oven (140 °C) and firing at 900 °C for 4 h.

3. Modified Columbite Method. For the modified columbite method, MgO in the form of $(MgCO_3)_4Mg(OH)_2{\cdot}5H_2O$ was used in a 2% excess. The $(MgCO_3)_4Mg(OH)_2{\cdot}5H_2O$ powder was

(35) Weil, J. A.; Bolton, J. R.; Wertz, J. E. *Electron Paramagnetic Resonance*; John Wiley & Sons: New York, 1994.
(36) Warren, W. L.; Robertson, J.; Dimos, D.; Tuttle, B. A.; Pike, G. E.; Payne, D. A. *Phys. Rev. B* **1996,** *53*, 3080.
(37) Warren, W. L.; Seager, C. H.; Dimos, D.; Friebele, E. J.*Appl. Phys. Lett.* **1992**, *61*, 2530.
(38) Seager, C. H.; Warren, W. L.; Tuttle, B. A.; Nasby, R. D.; Dimos, D. *Mater. Res. Soc. Symp. Proc.* **1993**, *284*, 493.
(39) Warren, W. L.; Tuttle, B. A.; Shwartz, R. W.; Hammetter, W. F.; Goodnow, D. C.; Evans, J. T., Jr.; Bullington, J. A. *Mater. Res. Soc. Symp. Proc.* **1993**, *310*, 3.
(40) Kutty, T. R. N.; Balachandran, R. Mater. *Chem. Phys.* **1985**, *13*, 467.
(41) Swartz, S. L.; Shrout, T. R.*Mater. Res. Bull.* **1982**, *17*, 1245.

mixed with Nb_2O_5 powder in an ethanol slurry and ground for 2 h. The resulting paste was dried in an oven (140 °C) overnight and fired at 1000 °C for 6 h. The precursor $MgNb_2O_6$ obtained by this method was mixed with PbO according to the PMN stoichiometry in ethanol for 1.5 h. Following a two-stage calcination process as summarized by Gupta and Kulkari,[14] the dried paste was fired first at 800 °C for 2 h. The resulting light yellow powder was mixed in an ethanol slurry again for 1 h, the solvent removed by oven drying (140 °C) overnight, and the powder fired at 900 °C for 2 h.

4. Wolframite Method.[42] This method initially involves the synthesis of a lead niobate precursor, $Pb_3Nb_2O_8$ (P_3N_2). PbO and Nb_2O_5 powders were mixed in an ethanol slurry, the solvent dried in an oven (140 °C) overnight, and the resulting powder fired at 820 °C for 4 h to yield orange-brown powders. The P_3N_2 product formed was then mixed with MgO (2% excess) in ethanol based on the PMN stoichiometry. The paste formed by this approach was dried in an oven (140 °C) overnight, fired at 830 °C for 3 h, reground in ethanol for 1 h, fired a second time at 830 °C for 3 h, reground in ethanol for 1 h, and finally fired at 900 °C for 4 h.

5. Molten Salt Method.[43] The starting materials $MgNb_2O_6$ (Alfa, 99.9%) and PbO were mixed with Li_2SO_4/Na_2SO_4 salt mixture in an ethanol slurry for 1.5 h. The ratio of the total weight of the salts to the total weight of the oxides was 0.5. The oven-dried paste (140 °C) was fired at 800 °C. The solid obtained was washed with a large quantity of distilled water to remove the soluble salts, and the resulting light yellow powders were dried in an oven (140 °C).

Synthesis of the PMN Pyrochlore Phase $Pb_{1.83}Nb_{1.71}Mg_{0.29}O_{6.39}$.[44] The starting materials PbO, Nb_2O_5, and MgO powders were mixed in an ethanol slurry for 1 h, dried in an oven (140 °C) overnight, and fired at 880 °C for 8 h.

Synthesis of 0.9 PMN/0.1 PT.[20−21,45] The 0.9 PMN/0.1 PT powder was prepared using the PMN powder obtained from the modified columbite method. This starting material was mixed with a corresponding ratio of TiO_2 in the anatase phase (Aldrich, 99.9+%) and PbO (Alfa, 99.9995%, 0.5% excess). The powder mixture was ground for 1 h in ethanol, dried of solvent in an oven (140 °C) overnight, and the resulting powder calcinated at 900 °C for 4 h.

Sample Annealing. PMN powders prepared by the molten salt method were annealed in a quartz tube under air and 5% hydrogen/95% nitrogen at 800 °C for 2 h, respectively, and under oxygen at 600 °C for 2 h.

Physical−Chemical Characterization Methods. *Power X-ray Diffraction Analysis.* Powder X-ray diffraction analysis was performed at the Engineering and Mining Experiment Station, South Dakota School of Mines and Technology, Rapid City, SD, using a PHILLIPS X-ray diffractometer. The samples were scanned using Cu Kα radiation ($\lambda = 1.54178$ Å) at 40 kV and 20 mA. The 2θ scan range was varied from 5° to 60° with scan speeds of 0.02 2θ degrees per step, 2 s per step.

Electron Paramagnetic Resonance (EPR) Measurements. EPR measurements were performed at the Department of Chemistry, University of New Hampshire. A home-assembled EPR spectrometer consisting of a Bruker microwave bridge and field controller, an Alpha magnet, a Varian magnet power supply, a PAR lock-in amplifier, a Micro-Now field modulation amplifier, and a Varian TE104 rectangular cavity was employed. The X-band spectra were recorded at 10 and 85 K using a Helitran flow system for He or N_2 gas as described elsewhere.[46] Q-band spectra were obtained with a Varian E−9 spectrometer and an E−110 microwave bridge fitted with a ribbon-wound cavity.[47] Samples were contained in 4 mm (o.d.) × 3 mm (i.d.) T08 quartz tubes.

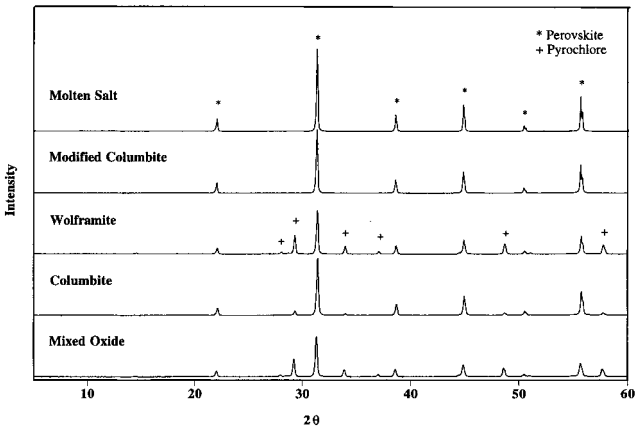

Figure 2. Powder XRD profile of PMN powders synthesized by different solid-state methods. The samples were scanned using Cu Kα radiation at 40 kV and 20 mA. The 2θ scan range was varied from 5° to 60° with scan speeds of 0.02° 2θ per step, at 2 s.

Table 1. Percentage of Perovskite Phase in PMN Powders Obtained by Different Solid-State Syntheses

synthetic method	percentage of perovskite[a]
mixed oxide method, 1% excess PbO, pellets, 900 °C, 4 h[14]	69
original columbite method, stoichiometric PbO, 900 °C, 4 h[41]	93
wolframite method, third firing, 2% excess MgO, 900 °C, 4 h[42]	70
modified columbite method, 900 °C, 2 h[14]	100
molten salt, 800 °C for 1.5 h[43]	100

[a] Estimate based on the measurement of the peak height of the most intense X-ray diffraction lines for the perovskite (110) and pyrochlore (222) phase of PMN samples.

Results and Discussion

PMN powders synthesized by various solid-state methods are known to contain variable contents of the PMN perovskite and pyrochlore crystalline phases based on powder XRD analysis.[14] Numerous synthetic methods and procedures have been reviewed for the solid-state reactions used to prepare PMN due to the deleterious effects of even minor pyrochlore phase contents on the dielectric properties of PMN.[14] The five solid-state methods studied here are representative of the solid-state reaction approaches currently used for the synthesis of PMN. The phase contents of the PMN samples prepared by these methods were determined from the XRD profiles as shown in Figure 2. The relative percentages of the perovskite phase content as estimated from measurements of the peak height of the most intense X-ray diffraction lines for the perovskite (110) and pyrochlore (222) phase of PMN samples are summarized in Table 1. The PMN materials synthesized by these five methods were found to contain varying contents of the PMN perovskite and pyrochlore crystalline phases. PMN powders prepared by the modified columbite method and the molten salt method were found to produce an XRD pure-phase PMN material of the perovskite lattice structure. The PMN products obtained by the other three methods were found to produce polycrystalline materials of variable

(42) Guha, J. P.; Anderson, H. U. *J. Am. Ceram. Soc.* **1986**, *69*, C287.
(43) Yoon, K. H.; Cho, Y. S.; Kang, D. H. *J. Mater. Sci.* **1995**, *30*, 4244.
(44) Shrout, T. R.; Swartz, S. L. *Mater. Res. Bull.* **1983**, *18*, 663.
(45) Yang, M. F.; Ling, H. C.; Rhodes, W. W. *J. Mater. Res.* **1989**, *4*, 930.
(46) Yang, X.; Chasteen, N. D. *Biophys. J.* **1996**, *71*, 1587.
(47) Wang, W.; Chasteen, N. D. *J. Magn. Reson.* **1995**, *116*, 237.

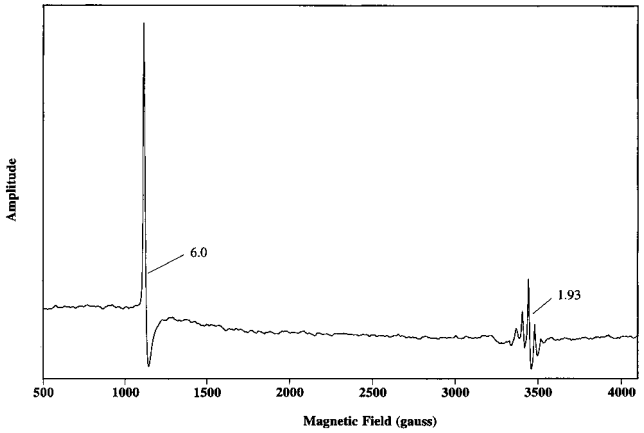

Figure 3. X-band EPR spectrum of $PbTiO_3$ (Alfa, 99.5%) powders recorded at 77 K; effective g values of paramagnetic species are indicated. Spectrometer parameters: microwave power, 1 mW; modulation amplitude, 0.3 G; time constant, 1.0 s; scan time, 500 s.

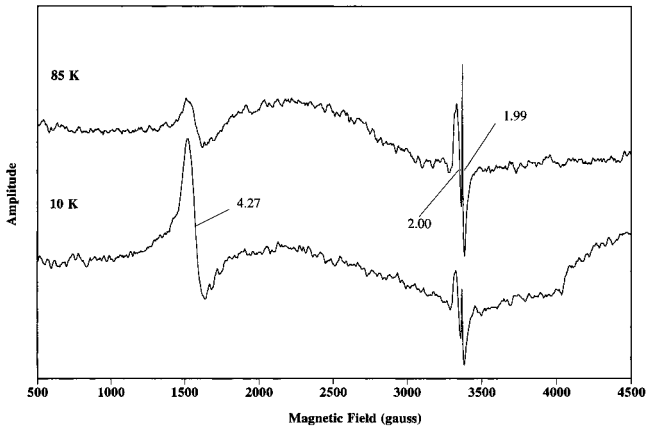

Figure 4. X-band EPR spectra of the PMN pyrochlore ($Pb_{1.83}Nb_{1.71}Mg_{0.29}O_{6.39}$) powder recorded at 10 and 85 K. Spectrometer parameters: microwave power, 0.5 mW; modulation amplitude, 2 G; time constant, 1.0 s; scan time, 500 s.

contents of PMN (69−93%) of the perovskite lattice structure (Table 1).

In the present study, EPR spectroscopy was used to measure the presence of several paramagnetic metal ion signals identified for adventitious Fe^{3+} ion species and/or reduced Ti^{3+} ion contained in the B-sites of PMN powders and the presence of oxidized Pb^{3+} ions in the A-sites of PMN powdered materials (see Figure 1). Correlations between the presence of these observed metal ion species from EPR measurements for PMN materials prepared by different synthetic approaches, as well as correlations that may be related to the perovskite/pyrochlore content of the PMN powders, were explored. Previous EPR studies of PMN materials containing added dopant Fe^{3+} ion as an EPR probe of the B-sites in these systems have shown several complications associated with higher level Fe^{3+} ion doping of PMN, including the difficulty in controlling sample homogeneity at higher levels of dopant present in the sample[27] and the occurrence of additional complex EPR features as observed at these higher Fe^{3+} ion dopant concentrations.[27,40] Previous EPR studies of PZT and PLZT systems have shown that the presence of paramagnetic Fe^{3+}, Pb^{3+}, and Ti^{3+} ion species in undoped samples can provide useful atomic-level information based on interpretation of the EPR signals for these systems.[48,49]

EPR Spectra of $PbTiO_3$ (PT) and the Pyrochlore PMN $Pb_{1.83}Nb_{1.71}Mg_{0.29}O_{6.39}$. Lead titanate ($PbTiO_3$) that is commonly used to prepare PMN/PT materials has been extensively studied by EPR since it is an important ferroelectric material and a component or reactant in the syntheses of many lead-based ferroelectric or piezoelectric systems of the perovskite lattice structure.[50] The X-band EPR spectrum of lead titanate obtained at 77 K is shown in Figure 3. The spectrum displays an intense signal at $g = 6.0$ that is assigned to the perpendicular component of an adventitious Fe^{3+} impurity located in the tetragonal (axial) B-sites. In addition, a composite series of resonances is seen near $g = 1.93$, typical of reduced Ti^{3+}.[37,51−54] The composite signal has contributions from $^{46,47,49,50}Ti$ isotopes[55−57] as well as the $g = 2$ parallel component of tetragonal Fe^{3+} ion.[35] However, the observed pattern of resonances cannot be accounted for by these signals alone. It is speculated that other signals near $g = 2$ from isotopes 204, 205, 207 and 208 of Pb^{3+} ions[58−62] and possibly from fine structure spectra of high-spin Fe^{3+} ion with a small zero-field splitting[35] may be contributing to the pattern. The present data do not permit distinction between these possibilities.

Lead magnesium niobate of the pyrochlore structure, $Pb_{1.83}Nb_{1.71}Mg_{0.29}O_{6.39}$, exists as a minor phase in many synthesized PMN powdered ceramics products.[63] The X-band EPR spectra of this material observed at 10 and 85 K are shown in Figure 4. These two spectra show similar EPR features, namely, an intense peak at ca. $g = 4.27$ assigned to Fe^{3+} ions of rhombic symmetry, a broad peak at $g = 2.00$, and an intense peak at $g = 1.99$. The broad signal at $g = 2.00$ is assigned to Pb^{3+} ion sites.[58−62] The sharp peak at $g = 1.99$ is assigned to ideal cubic symmetry Fe^{3+} ion sites.[28] The ratio of the amplitudes of the peaks due to the rhombic Fe^{3+} ion and the cubic Fe^{3+} ion centers decreases as the temperature increases from 10 to 85 K, consistent with greater electron relaxation in the rhombic site relative to the cubic site.

EPR Spectra of Lead Magnesium Niobate [Pb($Mg_{1/3}Nb_{2/3}$)O_3, PMN] Powders. The EPR studies of

(48) Warren, W. L.; Tuttle, B. A.; Rong, F. C.; Gerardi, G. J.; Poindexter, E. H. *J. Am. Ceram. Soc.* **1997**, *80*, 680.
(49) Seager, C. H.; Warren, W. L. *J. Appl. Phys.* **1993**, *73*, 7720.
(50) Hamada, K.; Senna, M. *J. Mater. Sci.* **1996**, *31*, 1725.
(51) Bykov, I. P.; Glinchuk, M. D.; Skorokhod, V. V.; Kurland, V. M. *Ferroelectrics* **1992**, *127*, 89.
(52) Abraham, M. M.; Bamberger, C. E. *J. Am. Ceram. Soc.* **1991**, *74*, 2299.
(53) Davies, J. J.; Wertz, J. E. *J. Phys. Chem. Solids* **1970**, *31*, 2489.
(54) Engelen, P. P. J. Van; Henning, J. C. M. *Phys. Lett.* **1967**, *25A*, 733.
(55) Castellano, F. N.; Stipkala, J. M.; Friedman, L. A.; Meyer, G. J. *Chem. Mater.* **1994**, *6*, 2123.
(56) Hiraki, K.; Inoue, T.; Hirai, H. *J. Polym. Sci.* **1970**, *A-1*, *8*, 2543.
(57) Schulz, H.-J.; Kreissl, J. *Opti. Mater.* **1995**, *4*, 202.
(58) Born, G.; Hofstaetter, A.; Scharmann, A.; Vitt, B. *Z. Physik B.* **1976**, *23*, 307.
(59) Abragam, A.; Bleaney, B. *Electron Paramagnetic Resonance of Transition Ions*; Dover Publications: New York, 1986.
(60) Popescu, F. F.; Grecu, V. V. *Phys. Stat. Sol. (b)* **1975**, *68*, 595.
(61) Nishi, M.; Hara, H.; Ueda, Y.; Kazumata, Y. *J. Phys. Soc. Jpn.* **1977**, *42*, 1900.
(62) Griscom, D. L. *J. Non-Crystalline Solids* **1980**, *40*, 211−272.
(63) Wakiya, N.; Saiki, A.; Ishizawa, N.; Shinozaki, K.; Mizutani, N. *Mater. Res. Bull.* **1993**, *28*, 137.

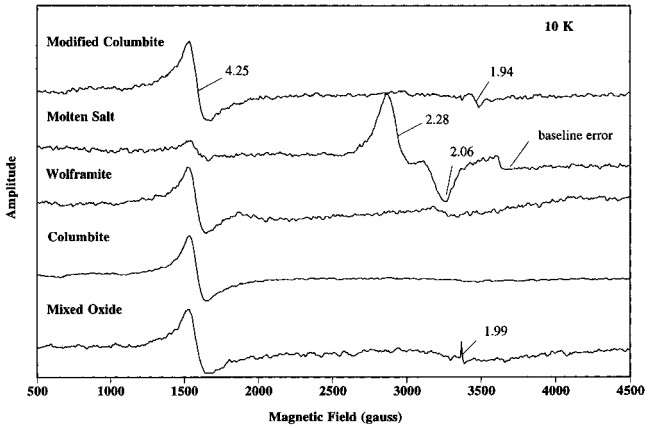

Figure 5. X-band EPR spectra recorded at 10 K for PMN powders synthesized by different solid-state methods. Spectrometer parameters: microwave power, 0.5 mW for samples from the mixed oxide and molten salt methods, 4 mW for samples from the original columbite and wolframite methods, and 2 mW for the sample from the modified columbite method; modulation amplitude, 2 G; time constant, 1.0 s; scan time, 500 s.

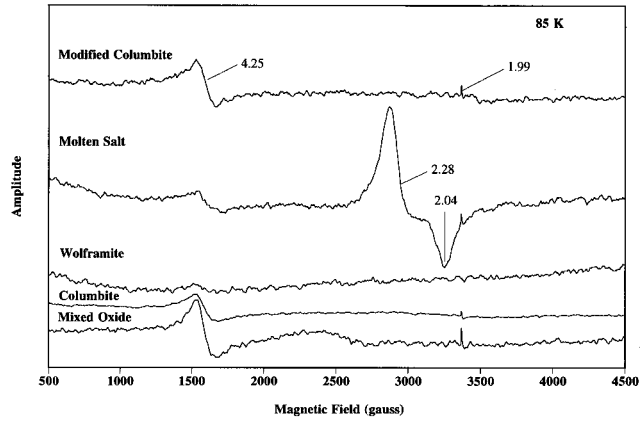

Figure 6. X-band EPR spectra recorded at 85 K for PMN powders synthesized by different solid-state methods. Spectrometer parameters: microwave power, 0.5 mW for the samples from the mixed oxide method, 5 mW for samples from the original columbite, 4 mW for the sample from the wolframite method, 3 mW for the sample from the molten salt method, and 2 mW for the sample from the modified columbite method; modulation amplitude, 2 G; time constant, 1.0 s; scan time, 500 s.

PMN reported here have examined polycrystalline powders that contain different contents of perovskite and pyrochlore phases of PMN (Figure 2 and Table 1). The X-band EPR spectra of the five PMN powders obtained at 10 and 85 K are shown in Figures 5 and 6, respectively. These EPR spectra exhibit three types of EPR signals: a $g = 4.25$ signal that is assigned to rhombic Fe^{3+} ion centers ($E/D \approx {}^1/_3$, $D > h\nu$), its amplitude decreasing as the temperature increases from 10 to 85 K (This signal decreases in amplitude at elevated temperature due to the Boltzmann factor and increased electron spin relaxation rate at higher temperatures.);[64] a $g = 1.99$ signal assigned to an ideal cubic Fe^{3+} ion center, its intensity increasing as the temperature increases from 10 to 85 K due to power saturation effects at low temperatures; and a $g = 2.2-2.3$ signal that is only observed in PMN prepared by molten salt

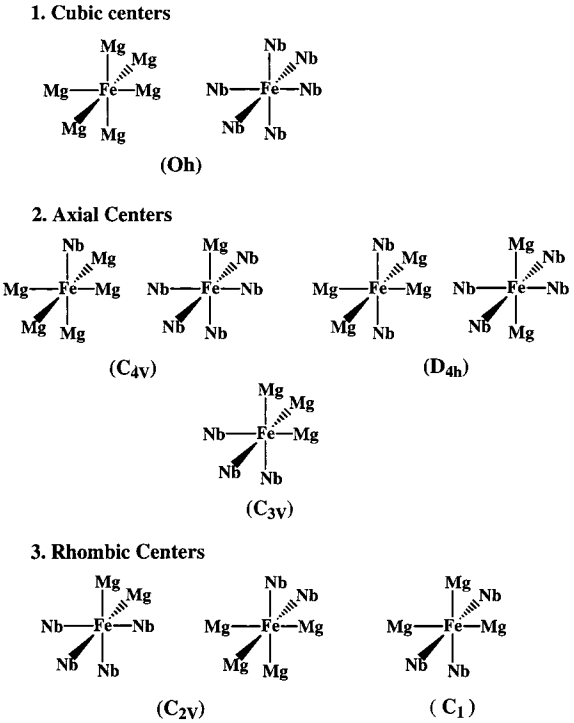

Figure 7. Symmetries of all possible configurations of next-nearest neighboring Mg/Nb for Fe^{3+} ions in the B-sites of substituted PMN.

method and is likely due to interstitial Fe(III) oxide or hydroxide phases[65] introduced or produced by this unique synthetic method or due to oxidized axial Pb^{3+} ion defect sites.

Powder XRD patterns of the various PMN powders studied here show an average cubic perovskite lattice structure based on the ideal lattice positions of the A- and B-site ions (see Figure 1). In discussing the short-range order of PMN systems, however, two possible mechanisms must be used to account for the reduction in the local symmetry of the adventitious Fe^{3+} ions that occupy the B-sites normally occupied by Nb^{5+} and Mg^{2+} ions in PMN perovskite lattice structure:[28] first, a temperature-dependent elastic displacement or ion motion of the B-site lattice ions may be occurring in the polar domain regions of the PMN materials, and second, the chemical structural disorder of the $Fe^{3+}/Mg^{2+}/Nb^{5+}$ ions in local domain regions of the PMN powders may lead to uncompensated charges due to the random distribution of the Mg^{2+}, Fe^{3+}, and Nb^{5+} ions in the B-sites of PMN.

Glinchuk et al. have calculated the theoretical EPR behavior for Fe^{3+} ions resulting from doping Fe^{3+} ion in the B-site of PMN for several different "next-nearest neighbor (nnn) B-site" configurations (Figure 7).[28] These different Fe^{3+} ion configurations of Fe−O−Mg(O−Nb) structural units as shown in Figure 7 may produce three different types of EPR signals from Fe^{3+} ($S = {}^5/_2$) ions contained as substituent ions for either the Nb^{5+} or the Mg^{2+} ions in the B-sites of PMN: (1) cubic sites ($D = E = 0$), where the six nnn B-site ions are all Mg or Nb; (2) axial sites ($E = 0$), containing two Mg(Nb) and four Nb-(Mg) nnn B-site ions, with two Mg(Nb) on the same axis; or three Nb and three Mg, with no Mg (Nb) ions in the

(64) Ayscough, P. B. *Electron Spin Resonance in Chemistry*; Methuen & Co Ltd.: London, 1967.

(65) Goldfarb, D.; Bernardo, M.; Strohmaier, K. G.; Vaughan, D. E. W.; Thomann, H. *J. Am. Chem. Soc.* **1994**, *116*, 6344.

same axis; or one Mg(Nb) and five Nb(Mg); and (3) rhombic sites ($D/E = 3$), containing three Mg and three Nb, with two Mg(Nb) on the same axis; or two Mg(Nb) and four Nb(Mg), with two Mg(Nb) ions not on the same axis. In their experimental EPR studies of Fe^{3+} ions in 0.1 mol % Fe_2O_3 doped-PMN ceramics prepared by a two-stage hot press method, all three types of EPR signals due to Fe^{3+} ion centers with these local site configurations and symmetries were observed. The magnetic field positions and line shapes of the observed EPR signals were found to be consistent with computer simulation results. Such correlations provided evidence to postulate that the Nb and Mg ions are not distributed in ordered cation configurations in the B-sites of the PMN system, leading to the occurrence of all possible Mg/Nb nnn B-site configurations, as shown in Figure 7. These reported EPR results and interpretations therefore provide little support for the "1:1 ordered" local B-site structural model for PMN of the perovskite lattice structure. In the experiments reported herein, however, the Fe^{3+} ion signal of axial symmetry is not observed in any of the undoped PMN samples from the various synthetic methods studied (see Figures 5 and 6), although this signal may occur below the detection limit of the EPR measurements. This axial Fe^{3+} ion signal is, however, readily observed in the spectrum of $PbTiO_3$ powders discussed above (Figure 3).

Dimza has conducted an EPR study of signals due to Fe^{3+} ion doped in PMN materials at variable concentration. When the Fe^{3+} concentration increased from 0.01 wt % to 0.1 and 1 wt %, the Fe^{3+} ion signal having an axial symmetry with $g_\perp = 6$, and $g_{||} \approx 2.0$ was observed.[27] Therefore, it is likely that the axial Fe^{3+} ion centers observed by Glinchuk et al. are a result of the relatively high dopant Fe^{3+} ion concentrations introduced in their PMN materials.[28] The observation of only Fe^{3+} ion EPR signals of rhombic and cubic symmetry for the synthesized PMN systems studied here indicates that there may be fewer possibilities for Mg/Nb nnn B-site configurations than depicted in Figure 7. Most importantly, the results reported here indicate that Fe^{3+} ion sites of axial symmetry (C_{3v}, C_{4v}, and D_{4h}) either are not present in PMN materials studied here or are of a much lower concentration than the B-site Fe^{3+} ions of cubic and rhombic symmetry. Therefore, a higher degree of short-range order likely exists for Fe^{3+} ions in the B-sites of PMN for these lower Fe^{3+} ion content materials studied here based on the EPR results at 10 and 85 K, far below its reported Curie temperature (258 K).

For the various PMN powders studied here, the PMN materials obtained by the molten salt method show the most unique EPR spectral features. Despite the nearly identical XRD patterns observed for the PMN powders prepared by the molten salt method and that of the PMN product obtained from the modified columbite method (Figure 2), their EPR spectra are strikingly different. The observed EPR spectral differences may be the consequence of several important differences related to these PMN materials: (1) the PMN powders may have different microstructures, as has been proposed for PMN materials prepared from different solid-state synthesis reactions,[14] or (2) the introduction of Fe^{3+} ion impurities or moisture during the aqueous

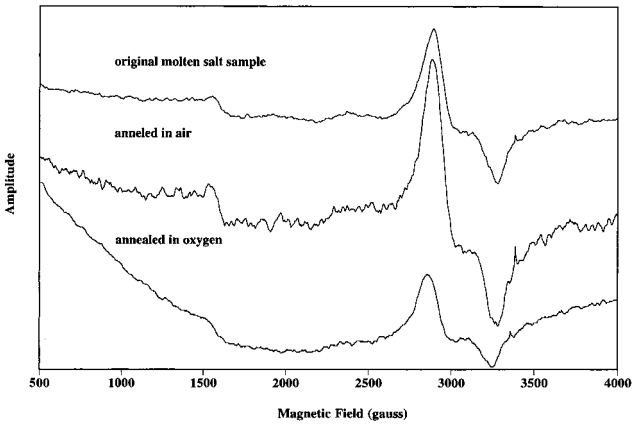

Figure 8. X-band EPR spectra recorded at 90 K for PMN powders synthesized by the molten salt method and treated under different annealing atmosphere at 800 °C and 2 h. Spectrometer parameters: microwave power, 3 mW; modulation amplitude, 2 G; time constant, 1.0 s; scan time, 500 s.

treatment of the final molten salt PMN product following final firing may lead to these EPR spectral differences, or (3) the introduction of additional paramagnetic species may occur during the molten salt synthesis process as a result of its unique starting material and salt composition. The most noticeable EPR signal for PMN prepared by the molten salt method is the band at $g = 2.30-2.28$ that exhibits a g value higher than the free electron g value (2.0023). One interpretation is that this signal is due to high-spin Fe^{3+} ion, since a $g = 2.3$ signal has been previously assigned to high-spin Fe^{3+} ions in a weak ligand field of water, hydroxide, and framework oxide local chemical environments.[65] The synthetic procedure used in the molten salt method may lead to the formation of such high-spin iron(III)−oxygen sites. Another possible interpretation, suggested from the line shape of the EPR bands in the $g = 2.3-2.0$ region, is that this signal is due to an axially compressed Pb^{3+} ion (d^9, $S = {}^1/_2$). In this case, spin−orbit coupling of the unpaired electron in the d_{z^2} orbital would result in the observed $g_\perp$ value (2.28) being much larger than the free electron value (2.0023) and the $g_{||}$ value (2.04) being close to 2.0023, as observed here.

To assess this latter interpretation for the EPR signal at $g = 2.28$, PMN samples prepared by the molten salt were annealed in an air and oxygen atmosphere at 800 °C, respectively, while an additional PMN sample was annealed in a hydrogen/nitrogen atmosphere at 600 °C for 2 h. The X-band EPR spectra taken at 90 K for the annealed PMN samples (air and oxygen), and the original PMN sample are shown in Figure 8. These spectra indicate that the shape and positions of the EPR resonances observed for PMN samples treated by annealing under pure oxygen oxidizing conditions do not change appreciably, thus excluding the possibility that either oxygen vacancies or high-spin ferric ion sites associated with water or hydroxide ligands produce the EPR band at $g = 2.2-2.3$. The PMN sample annealed under reducing atmospheres, however, loses all EPR resonance features (data not shown). Although the reduction treatment is not highly selective for any of the paramagnetic species present in PMN, the results are consistent with the presence of Pb^{3+} ion sites in PMN. On the basis of the results of these annealing experiments, the EPR band observed at $g_\perp = 2.28$ and

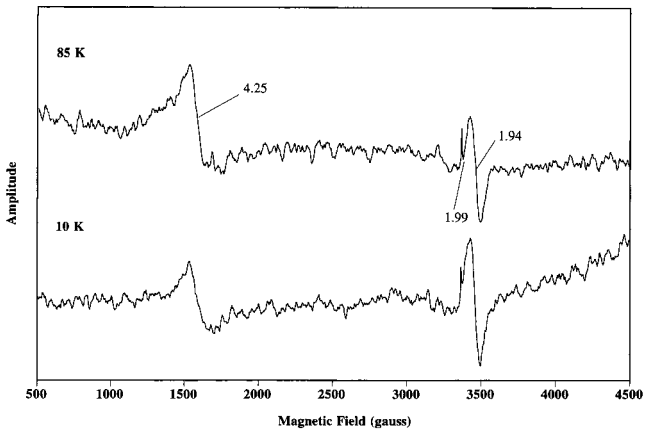

Figure 9. X-band EPR spectra recorded at 10 and 85 K for the 0.9 PMN/0.1 PT powder. Spectrometer parameters: microwave power, 2 mW; modulation amplitude, 2 G; time constant, 1.0 s; scan time, 500 s.

$g_{||} = 2.04$ in PMN powders prepared by the molten salt method is most reasonably assigned to Pb^{3+} ions (d^9) of axial symmetry in the A-sites of PMN. A similar EPR signal at $g = 2.167$ that has been assigned to the Pb^{3+} ion has also been reported for low Pb dopant ions in ZnTe semiconductors.[66]

EPR studies at the Q-band were also performed on PMN samples obtained by the modified columbite and molten salt methods to further explore the various EPR features and their peak assignments discussed previously. Unfortunately, considerable microheterogenity (site variation) is present in the PMN samples that causes frequency (*g*-strain) broadening at the higher field (~12 500 G) strength used for the Q-band measurements. Therefore, no EPR spectral features were observed in Q-band measurements. Such observations, however, are consistent with the broad resonance lines observed in the various X-band EPR spectra for the PMN materials discussed earlier.

An additional X-band EPR signal at $g = 1.94$ is observed for the PMN sample obtained by the modified columbite method at 10 and 85 K. The origin of this EPR signal is uncertain and could be due to trace ions or reduced Nb^{4+} ions.

EPR Spectra of PMN/PT Solid Solution Powders. In addition to the EPR studies reported here for various PMN powders, the EPR spectra of a 0.9 PMN/0.1 PT solid solution powder were also examined at 10 and 85 K (Figure 9). The X-band spectra of the 0.9 PMN/0.1 PT powder obtained at these temperatures are very similar in appearance to the corresponding EPR spectra observed for the PMN powders obtained by the modified columbite method. The latter PMN powder was used as a starting material for the synthesis of the PMN/PT powder examined here. At both temperatures of measurement, a broad EPR signal at $g = 4.25$ and a sharp signal at $g = 1.99$ are observed. The former resonance is assigned to Fe^{3+} ions of rhombic symmetry and the latter to Fe^{3+} ions of cubic symmetry in the B-sites of the PMN/PT material. An intense EPR signal at $g = 1.94$ was also observed and is assigned to the Ti^{3+} ion. The higher amplitude of this signal is attributed to the formation of a higher content of B-site Ti^{3+} ion centers in the PMN/PT powder studied following the high-temperature (900 °C) reaction of PMN with PT to form this PMN/PT solid-solution material.

Conclusion

The EPR studies reported here have demonstrated that EPR is an important spectroscopic technique for examining the short-range order that exists in PMN powders prepared from different solid-state synthetic methods and for PMN/PT solid solution materials. The relationships between the EPR behavior of the various PMN materials and their different synthetic conditions have been described. X-band EPR spectra obtained at 10 and 85 K for PMN powders prepared by different synthetic methods and several related compounds have been observed to exhibit several important EPR signals: at $g = 1.99$ there is a narrow resonance, due to ideal cubic Fe^{3+} ion centers in the B-sites without any Fe^{3+} ion fluctuations or motion; at $g_{\perp} = 2.27-2.30$, $g_{||} = 2.04-2.06$ there is a broad, anisotropic signal, due to axial Pb^{3+} ion centers in the A-sites; and, at $g = 4.25$ there is a broad signal, due to rhombic Fe^{3+} ion center in the B-sites.

The appearance and intensities of the EPR signals observed for PMN materials were found to vary with temperature. The EPR signals for PMN powders prepared by different methods of syntheses were also observed to be substantially different.

In the work reported here, EPR signals were only observed for Fe^{3+} ions of the rhombic and cubic symmetry located in the B-sites of PMN and PMN/PT powders. These EPR results observed for Fe^{3+} ion as a probe of the B-sites in PMN indicate that there are fewer possibilities of Mg/Nb nnn B-site configurations, (i.e., no axial configurations) than a totally random distribution of Mg/Nb configuration would predict. Therefore, an intermediate degree of short-range order is observed for the Mg/Nb local nnn B-site configurations that exist in PMN powders examined below their Curie temperature (258 K), although it is difficult to provide a quantitative estimate from these EPR studies of the extent of B-site cation order that contributes to the local chemical structure of PMN.

The very unique EPR feature observed at $g = 2.0-2.3$ for PMN powders prepared by the molten salt method also indicates that this PMN material may have a different microstructure than PMN materials prepared by the other solid-state reaction methods. A study of the electrical properties of PMN powders prepared by the molten salt synthesis as well as PMN ceramics obtained by these other methods of synthesis is in progress to examine their effect on the dielectric behavior of these PMN materials.

Acknowledgment. The authors would like to acknowledge Mr. Michael Benjamin of SDSU for his initial synthetic work on PMN synthesis and Dr. Xiaoke Yang of UNH for the EPR measurements. Financial support for this work has been provided by the Department of Defense University Research Initiative Support Program (URISP, J.J.F.) through the Office of Naval Research (Grant No. N00014-96-1-0781). Funding for the construction of the X-band EPR spectrometer was provided by the National Institute of General Medical Science (Grant No. R37 GM20194).

(66) Suto, K.; Aoki, M. *J. Phys. Soc. Jpn.* **1967**, *22*, 1307.

CM980206N